ISSN 1392–1320 MATERIALS SCIENCE (MEDŽIAGOTYRA). Vol. 21, No. 1. 2015

Stress Induced Nitrogen Diffusion In Nitrided CoCr Alloy

Akvilė PETRAITIENĖ [1]*, Arvaidas GALDIKAS [1, 2], Teresa MOSKALIOVIENĖ [1]

[1] *Physics Department, Kaunas University of Technology, Studentų St. 50, LT-51368 Kaunas, Lithuania*
[2] *Department of Physics, Mathematics and Biophysics, Lithuanian University of Health Sciences, Eivenių 4, LT–50166 Kaunas, Lithuania*

crossref http://dx.doi.org/10.5755/j01.ms.21.1.5711

Received 13 November 2013; accepted 22 February 2014

In the present study the nitrogen transport mechanism in plasma nitrided CoCr alloy at moderate temperature (400 ºC) is explained by non-Fickian diffusion model. This mechanism is considered by stress induced diffusion model. The model involves diffusion of nitrogen induced by internal stresses created during nitriding process. The model considers the diffusion of nitrogen in the presence of internal stresses gradient induced by penetrating nitrogen as the next driving force of diffusion after concentration gradient. This model is commonly used for analysis of stainless steel nitriding; however, in this work it is shown that the same nitrogen penetration mechanism takes place in CoCr alloy. For mathematical description of stress induced diffusion process the equation of baro-diffusion is used which involves concentration dependent baro-diffusion concentration.

For calculation of stress gradient it is assumed that stress depth profile linearly relates with nitrogen concentration depth profile. The fitting is done using experimental curves of nitrogen depth profiles for medical grade CoCr alloy (ISO 5831-12) nitrided at 400 ºC temperature. The experimental curves are taken from literature. The nitriding duration was 2 h, 6 h, 20 h. The calculated nitrogen depth profiles in CoCr alloy are in good agreement with the experimental nitrogen depth profiles. The diffusion coefficient D is found from fitting of experimental data.
Keywords: CoCr alloy; nitriding; concentration dependent diffusion; kinetic modeling.

INTRODUCTION

CoCrMo alloys are widely used for orthopedic applications such as hip and knee joint replacements [1 – 4] due to their excellent corrosion and wear resistances. The highly biocompatibility of CoCr alloy is related closely to the excellent wear and corrosion resistance, imparted by a thin passive oxide film [2]. In general, with about 26 wt. % – 30 wt. % of chromium, it exhibits a very high resistance to corrosion by a thin passive oxide Cr_2O_3 film formed spontaneously on the alloy surface [1]. There is a strong demand to improve the mechanical reliability of biomedical metallic materials to realize orthopedic implants with long lifetimes. Consequently, much effort has been made to enhance alloy design and optimize hot deformation CoCrMo alloys [5].

It is known that surface treatments are applied to produce coatings or protective layers to increase the wear resistance and reduce the possibility of implant failure and osteolysis. As one of the important surface strengthening processes, nitrogen ion implantation has shown to improve wear resistance of orthopedic components such as the knee and hip replacements [1, 2, 5]. Nitriding of CoCr alloys has been reported to improve wear resistance, typically showing an increase of the surface hardness to (15 – 20) GPa in combination with a wear rate reduced by a factor of 10 – 100 [6]. These improved mechanical properties are caused by the insertion of up to 35 at. % nitrogen in the near surface region, extending up to 10 μm below the surface [6].

In order to conserve the intrinsic good corrosion resistance, the nitriding has to avoid CrN precipitates on layer formation. Low-temperature plasma nitriding and carburizing can improve the surface hardness and tribological properties of austenite stainless steel without losing its corrosion resistance by forming C or N supersaturated face – centered cubic (fcc) expanded austenite phase, so called S-phase [7 – 9]. Recently, Dong et al. have discovered that S-phase can be generated in Co-Cr alloys by low-temperature plasma surface alloying with nitrogen (nitriding) to improve the corrosion – wear resistance of Co-Cr alloys at very low temperatures (between 300 °C and 400 °C) [7].

The profiles of nitrogen exhibit plateau – type shapes with a very high concentration slightly decreasing in the γ_N layer and followed by a sharp decrease and a tail in the bulk, are not coherent with a simple diffusion-limited incorporation (erfc. shape) [9, 10]. As experimentally observed, the transport of nitrogen in CoCrMo alloy is non-Fickian, so understanding of nitrogen diffusion mechanisms in CoCrMo alloys is of great importance. To explain the such shape of nitrogen depth profiles several models were proposed: 1) the trapping-detrapping model [11, 12] proposed by Parascandola and co-workers; 2) the model based on Fick‘s laws and nitrogen diffusion coefficient dependence on nitrogen concentration [13]; 3) the model, based on nitrogen diffusion coefficient dependence on nitrogen concentration and trapping, i. e. the strong affinity between chromium and nitrogen [14, 15] and 4) the model, based on residual stresses and distortions [16].

As mentioned above, nitrogen insertion in to CoCrMo alloy leads to the formation of expanded austenite [6]. With the γ_N phase in the CoCrMo alloy the large lattice expansions (up to 10 %) is associated [17]. Such values are quite likely to induce compressive stresses in the γ_N layers [17]. The expansion of the lattice after nitrogen insertion is

*Corresponding author. Tel.: +370-606-85137, fax: +370-37-456472.
E-mail address: *apetraitiene@yahoo.com* (A. Petraitienė)

observed as a consequence of biaxial stress within the substrate [18]. When measuring the stress in situ during nitrogen implantation, a fast increase towards a plateau near the yield strength of 1.5 GPa was reported [19]. The stress gradient must be present to accommodate the transition between the expanded lattice and the substrate, which additionally leads to changes in the profile shape [18].

The main aim of this work is to propose the model, based on proposition that the transport of nitrogen in CoCrMo alloy is driving by stress gradient created during nitriding process.

THE MODEL

The stress induced nitrogen diffusion model is based on the fact that the incorporation of nitrogen into CoCr alloy causes lattice expansion which induces local internal stresses in matrix. Originally this model first was approved for analysis of chemical potential of hydrogen diffusing in self-stressed isotropic elastic metal [20 – 22]. The same expression of chemical potential was applied for diffusing nitrogen in stainless steel [23, 24]. According to Ref. [23, 24] described model will be used for analysis of nitrogen diffusivity in CoCr alloy.

In general case the diffusion flux is expressed by the gradient of component chemical potential $\mu(C, T, p)$:

$$J = -D\nabla\mu(C,T,p)\,, \tag{1}$$

where D is diffusion coefficient. Chemical potential is the function of concentration C, temperature T and pressure p. If temperature gradient does not exist the Eq. (1) can be expressed as:

$$J = -D(\nabla C + k_p \nabla p)\,. \tag{2}$$

This equation involves Fickian diffusion and baro-diffusion driving by the pressure p. Pressure p for solids is related with stress tensor $\sigma = \sigma_{xx} + \sigma_{yy} + \sigma_{zz}$ induced by the presence of nitrogen in the alloy. Stress factor k_p is expressed (Eq. (25) in Ref. [20]) as $k_p = V_N C / RT$, k_p represents the elastic part of the chemical potential gradient. It describes the stress-induced diffusion (SID). R = 8.314 m^3 Pa K^{-1} mol^{-1} is the gas constant.

The chemical potential of nitrogen μ as a mobile component in the CoCr alloy matrix depends on nitrogen concentration C and mechanical stress σ (Eq. (21) in Ref. [21]):

$$\mu = \mu(0,C) - V_N\sigma\,, \tag{3}$$

where μ(0,C) is the chemical potential in the stress-free state and V_N is the nitrogen partial molar volume. For CoCr alloy $V_N = 3.79\times10^{-6}$ m^3 mol^{-1} [25].

The equation of the nitrogen diffusion in presence of internal stress is expressed as:

$$J = -D\left(\nabla C - \frac{V_N C}{RT}\nabla\sigma\right). \tag{4}$$

Assuming that V_N and D do not depend on concentration the following equation of the nitrogen concentration variation from Eq. (4) can be expressed as:

$$\frac{\partial C(x,t)}{\partial t} = D\nabla\left(\nabla C(x,t) - \frac{V_N(x,t)\cdot C(x,t)}{RT}\nabla\sigma(x,t)\right). \tag{5}$$

The boundary conditions involving flux of nitrogen from outside to the surface can be written as:

$$\frac{\partial C(0,t)}{\partial t} = \frac{\alpha\cdot i_0}{N_{surface}}(N_0 - C(0,t)) + D\nabla\left(\nabla C(0,t) - \frac{V_N(0,t)}{RT}\nabla\sigma(0,t)\right). \tag{6}$$

The first term of this equation is the adsorption term, which describes the process of nitrogen adsorption on the surface, where i_0 is relative flux of nitrogen, α is the sticking coefficient of nitrogen to the surface atoms, N_0 is host atoms atomic density and $N_{surface}$ is the surface concentration of host atoms.

In order to solve Eqs. (5) and (6) the stress profile σ_x has to be defined. The stress-depth profile σ_x, induced by a composition profile is obtained from Eq. (15) in Ref. [26]):

$$\sigma_x = \frac{\beta E}{1-\nu}(\overline{C_N} - C_N(x))\,, \tag{7}$$

where β is Vegard's constant for nitrogen, E the Young's modulus of alloy, ν the Poisson's constant and $\overline{C_N}$ is average nitrogen content in the sample. In Ref. [26] it was shown that for nitriding of alloy the linear dependence on compositionally induced compressive stress on concentration (Eq. (18) in Ref. [26]) can be expresses as:

$$\sigma(x,t) = -X_{stress}C_{nitrogen}(x,t)\,, \tag{8}$$

where value of X_{stress} was taken as X_{stress} = 200 MPa (at. %)$^{-1}$. According to the similarity of such values as Young's modulus of steel (200.4 GPa) and of CoCr alloy (210 GPa [28]), Poisson's constants (ν = 0.33 for steel and ν = 0.3 for CoCr alloy [27]) and Vegard's constant β = 0.0080 Å (at. %)$^{-1}$ N for steel and CoCrMo alloy, we also will use this value for calculation.

The Eqs. (5) and (6) for one dimensional case expressed in finite increments obtain the following form [23, 24]:

For surface layer k = 0

$$\frac{\partial C^{(k)}}{\partial t} = \frac{\alpha\cdot i_0}{N_{surface}}(N_0 - C^{(k)}) + \frac{D}{h^2}\cdot\left[\left(C^{(k+1)} - C^{(k)}\right) - \frac{V_N}{RT}\left(C^{(k+1)}\left(\sigma^{(k+1)} - \sigma^{(k)}\right)\right)\right] \tag{9}$$

and for other layers k > 0

$$\frac{\partial C^{(k)}}{\partial t} = \frac{D}{h^2}\cdot\left[\left(C^{(k+1)} + C^{(k-1)} - 2C^{(k)}\right) - \frac{V_N}{RT}\left(C^{(k+1)}\left(\sigma^{(k+1)} - \sigma^{(k)}\right) + C^{(k)}\left(\sigma^{(k-1)} - \sigma^{(k)}\right)\right)\right], \tag{10}$$

where h is the thickness of one monolayer.

RESULTS AND DISCUSSION

The experimental results were analyzed by the proposed model. The experimental depth profiles of nitrogen taken from Ref. [17] and obtained by GDOES after plasma nitriding of CoCrMo alloy (medical grade alloy D30, ISO 5832-12) at 400 °C for different nitriding times 2 h, 6 h and 20 h are presented in Fig. 1 (points). The alloy was nitrited in a low-pressure (~ 60 mTorr) radio-frequency plasma under a gas mixture of 60 % N_2 – 40 % H_2 [17].

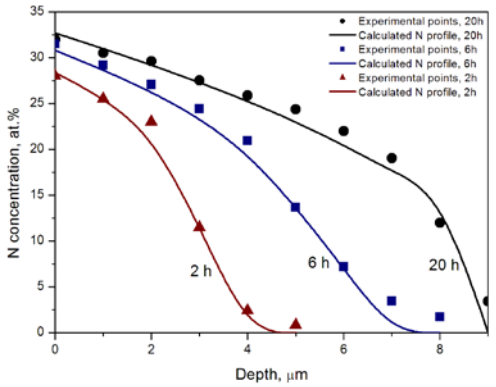

Fig. 1. Experimental (points) [17] and calculated (lines) nitrogen concentration depth profiles obtained at different nitriding times (2 h, 6 h and 20 h)

The plateau is seen in all curves, which cannot be fitted by simple diffusion models. The similar types of profiles for nitrided stainless steel are fitted by stress induced diffusion model [23, 24]. We suggest the same mechanism for CoCrMo alloy.

The nitrogen depth profiles in CoCrMo were calculated by solving Eqs. (9)–(10). In order to fit experimental curves the calculations were performed by varying diffusion coefficient *D*. Other parameters were kept as constants and found from experiment [17] or literature data [25–28]. Those parameters are listed in Table 1.

Table 1. The values of parameters used in calculations

The parameters from the literature [25–27]	Parameters found by fitting
X_{stress} = 200 MPa (at. %)$^{-1}$ R = 8.314 m^3 Pa K^{-1} mol^{-1} V_N = 3.79×10^{-6} m^3 mol^{-1} T = 673 K N_0 = 5.138×10^{21} cm^{-3}	Diffusion coefficients:

Nitriding time, h	D, ×10^{-11} cm^2 s^{-1}
2	1.89
6	1
20	0.7

The calculation results are presented in Fig. 1 (solid lines) together with the experimental points [17]. All three calculated depth profiles (2 h, 6 h and 20 h of nitriding) are in a good agreement with experimental points. However, in order to get the best fit for all three experimental depth profiles it was necessary to change diffusion coefficient (other parameters remain as constants for all three cases). The best fitting results were obtained with the following diffusion coefficients, listed in Table 1. It is seen from obtained values of diffusion coefficients that they decrease with increase of nitriding time. This may be influenced by concentration of nitrogen. With the increase of nitriding time the concentration of nitrogen increases and it means that diffusion coefficient decreases with increase of nitrogen concentration.

According to the Einstein-Smoluchowski relation the diffusion coefficient is inversely proportional to the nitrogen concentration [29]. To check Einstein-Smoluchowski relation for our case, the obtained values of diffusion coefficients were plotted versus parameter $1/C_N$ (C_N is total nitrogen concentration in sample). The plot is presented in Fig. 2.

All three points are in one line, which confirms assumption that diffusion coefficient depends on concentration according to Einstein-Smoluchowski relation as function $D \propto 1/C_N$.

The line of Fig. 2 is fitted by function:

$$D(C_N) = 3 \cdot 10^{11} / C_N - 8 \cdot 10^{-14}. \quad (11)$$

Analyzing the dependence of total nitrogen concentration on time (from Fig. 1) it was found the following function:

$$C_N(t) = 1.265 t^{0.429}. \quad (12)$$

Combining the last two relations the dependence of diffusion coefficient on time can be expressed as:

$$D(t) = 2.372 \cdot 10^{-11} t^{-0.4231} - 8 \cdot 10^{-14} \quad (13)$$

(for the experimental conditions described above). Using these expressions (Eqs. (11)–(13)) the depth profiles of nitrogen and stress profiles for any nitriding duration can be calculated.

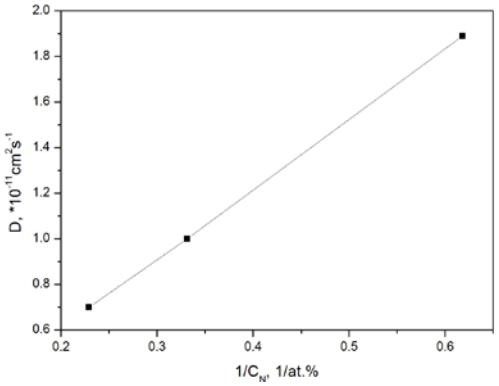

Fig. 2. Function of obtained by fitting D_o values versus $1/C_N$

The calculated stress profiles extracted from fitted data are presented in Fig. 3. It is seen that the increasing the nitrogen duration, the internal stresses increase.

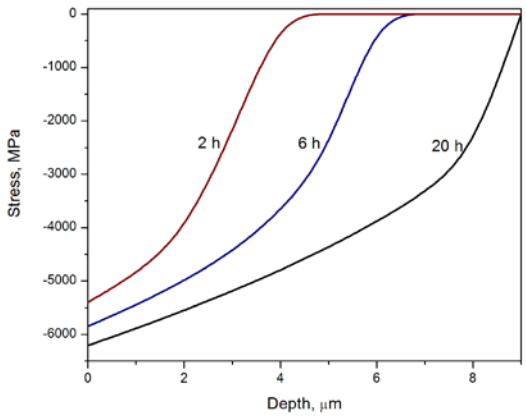

Fig. 3. The calculated (Eqs. (9) and (10)) stress profiles in nitrided CoCrMo alloy at 400 °C for 2, 6 and 20 h, calculated with different diffusion coefficients values, listed in Table. 1

By using Eqs. (11)–(13) the diffusion coefficients can be determinate for any nitriding time. The diffusion coefficients, listed in Table 1 are in good agreement with the experimental results, published in Ref. [27], where diffusions coefficients were calculated for the same CoCrMo alloy, nitrided in the same conditions – the average nitrogen diffusion coefficients were obtained from 1.131×10^{-11} to 1.81×10^{-11} cm^2 s^{-1} [27]. The determination of diffusion coefficient at any nitriding duration allows to calculation of depth profiles (Fig. 4) and stress profiles

(Fig. 5) for any nitriding durations. The calculated nitrogen depth profiles at different moments of time including the initial stage are presented in Fig. 4. It is seen that at initial stages of nitriding shape of curve is *erfc* type, i. e. the same as for simple diffusion. Up to ~10 min of nitriding nitrogen depth profiles are *erfc* type. At later nitriding stages (approximately after 10 min. Fig. 4) the shapes of curves begin to change, and after about $t = 30$ min of nitriding the plateau starts to be observed. The compressive stresses are induced by the lattice expansion, which are reliant on incoming nitrogen concentration. As mentioned previously, the nitrogen concentration in CoCrMo alloy is dependent on nitriding time. It is seen in Fig. 5 that at initial stage of nitriding internal stresses are small.

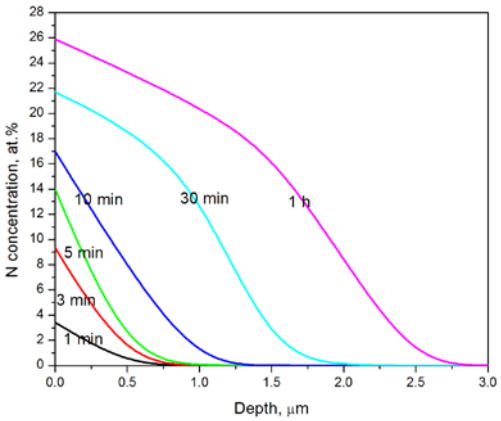

Fig. 4. The calculated (Eqs. (9)–(13)) nitrogen depth profiles at different nitriding durations

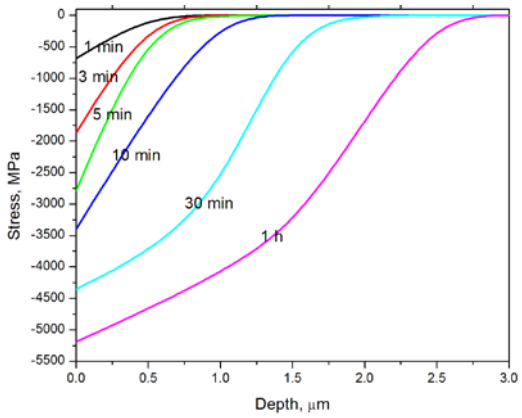

Fig. 5. The calculated (Eqs. (9)–(13)) nitrogen depth profiles at different nitriding durations.

The analysis of stress induced diffusion model shows a great important of the stresses influence to nitrogen distribution in to CoCrMo alloy. The stress is described by the stress factor X_{stress} (Eq. (8)), which value $X_{stress} = 200$ MPa (at.%)$^{-1}$ was proposed in Ref. [23, 24, 26]. The influence of the stress factor X_{stress} for nitrogen depth profiles is analyzed in Fig. 6. The nitrogen concentration and depth profiles are calculated with value of D obtained from fitting of the experimental results (Fig. 1) $D = 7\times10^{-12}$ cm^2 s^{-1} for 20 h nitriding duration with different X_{stress} values: 100 MPa (at.%)$^{-1}$, 150 MPa (at.%)$^{-1}$, 200 MPa (at.%)$^{-1}$. With increase of X_{stress} the nitrogen concentration slightly reduces on the surface but the variation of X_{stress} strongly influences the profile of nitrogen at deeper layers (shown in Fig. 6). The influence of the stress factor X_{stress} for stresses profiles is analyzed in Fig. 7. It is seen from Fig. 7 that the internal stresses and thickness of stressed layer increase with increase of X_{stress}. From those results it follows that diffusion process is more intensive as the internal stresses are higher.

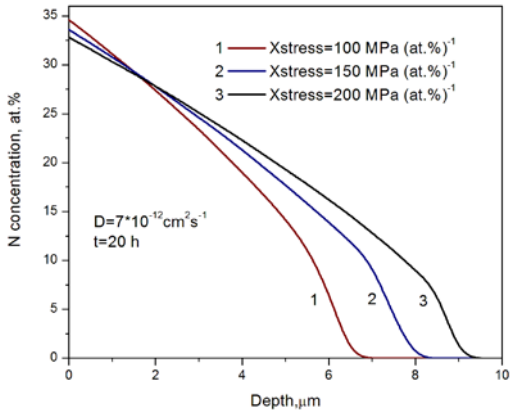

Fig. 6. The nitrogen depth profiles calculated (Eqs. (9)–(10)) for different values of stress factor X_{stress}. The nitriding time is 20 h and diffusion coefficient is 7×10^{-12} cm^2 s^{-1}

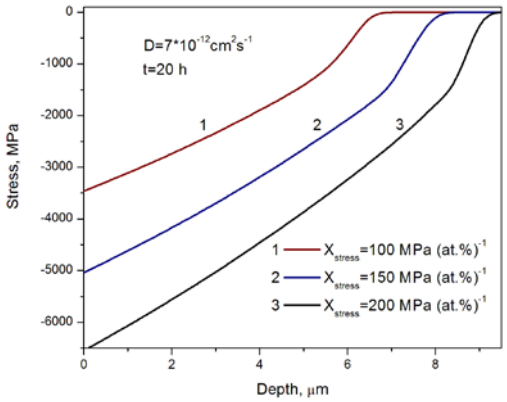

Fig. 7. The stress profiles calculated (Eqs. (9)–(10)) for different values of stress factor X_{stress}. The nitriding time is 20 h and diffusion coefficient is 7×10^{-12} cm^2 s^{-1}

CONCLUSIONS

1. The nitrogen penetration during plasma nitriding of CoCrMo alloy can be explained by stress induced diffusion mechanism and nitrogen depth profile can be calculated by this model.

2. The nitrogen diffusion coefficient in nitrided CoCrMo alloy depends on nitrogen concentration according to Einstein- Smoluchowski relation $D \propto 1/C_N$. Availing Einstein-Smoluchowski relation were derived equations showing the relationship between the nitridation time, the nitrogen concentration and the diffusion coefficient. These calculations allow to determinate the nitrogen concentration and diffusion coefficient for any nitriding duration.

3. According to the analysis of initial stage of nitriding it is seen that the plateau starts to be observed after about 30 min of nitriding duration. Until this time nitrogen depth profiles are erfc type – this is can be explained by small internal stresses at initial stages of nitriding.

4. The analysis of the internal stresses, formed in CoCrMo alloy during nitriding, shows that diffusion process is more intensive as the internal stresses are higher. The penetration depth of nitrogen increases with increasing of stress factor X_{stress}.

Acknowledgments

This research was funded by a grant (No. MIP-030/2013) from the Research Council of Lithuania.

REFERENCES

1. **Wang, Q., Zhang, L., Dong, J.** Effects of Plasma Nitriding on Microstructure and Tribological Properties of CoCrMo Alloy Implant Materials *Journal of Bionic Engineering* 7 2010: pp. 337 – 344.
2. **Wang, Q., Huang, C., Zhang, L.** Microstructure and Tribological Properties of Plasma Nitriding Cast CoCrMo Alloy *Journal of Materials Science and Technology* 28 (1) 2012: pp. 60 – 66. http://dx.doi.org/10.1016/S1005-0302(12)60024-3
3. **Sonntag, R., Reinders, J., Kretzer, J. P.** What's Next? Alternative Materials for Articulation in Total Joint Replacement *Acta Biomaterialia* 8 2012: pp. 2434 – 2441.
4. **Antunes, R. A., de Oliveira, M. C. L.** Corrosion Fatigue of Biomedical Metallic Alloys: Mechanisms and Mitigation *Acta Biomaterialia* 8 2012: pp. 937 – 962. http://dx.doi.org/10.1016/j.actbio.2011.09.012
5. **McGrory, B. J., Ruterbories, J. M., Pawar, V. D., Thomas, R. K., Salehi, A. B.** Comparison of Surface Characteristics of Retrieved Cobalt-Chromium Femoral Heads With and Without Ion Implantation *Journal of Arthroplasty* 27 2012: pp. 109 – 115.
6. **Mändl, S., Diaz, C., Gerlach, J. W., Garcia, J. A.** Near Surface Analysis of Duplex PIII Treated CoCr Alloys *Nuclear Instruments and Methods in Physics Research B* , 307 2013: pp. 305 – 309. http://dx.doi.org/10.1016/j.nimb.2012.11.052
7. **Liu, R., Li, X., Hu, X., Dong, H.** Surface Modification of a Medical Grade Co-Cr-Mo Alloy by Low-Temperature Plasma Surface Alloying with Nitrogen and Carbon *Surface and Coatings Technology* 232 2013: pp. 906 – 911.
8. **Christiansen, T. L., Drouet, M., Martinavicius, A., Somers, M. A. J.** Isotope Exchange Investigation of Nitrogen Redistribution in Expanded Austenite *Scripta Materialia* 69 2013: pp. 582 – 585.
9. **Pichon, L., Okur, S., Ozturk, O., Riviere, J. P., Drouet, M.** CoCrMo Alloy Treated by Floating Potential Plasma Assisted Nitriding and Plasma Based Ion Implantation: Influence of the Hydrogen Content and of the Ion Energy on the Nitrogen Incorporation *Surface and Coatings Technology* 204 2010: pp. 2913 – 2918.
10. **Lutz, J., Mändl, S., Lehmann, A.** Nitrogen Diffusion in Medical CoCrNiW Alloys After Plasma Immersion Ion Implantation *Surface and Coatings Technology* 202 2008: pp. 3747 – 3753. http://dx.doi.org/10.1016/j.surfcoat.2008.01.020
11. **Parascandola, S., Möler, W., Williamson, D. L.** The Nitrogen Transport in Austenitic Stainless Steel at Moderate Temperatures *Applied Physics Letters* 76 2000: p. 2194.
12. **Möller, W., Parascandola, S., Telbizova, T., Günzel, R., Richter, E.** Surface Processes and Diffusion Mechanisms of Ion Nitriding of Stainless Steel and Aluminum *Surface and Coatings Technology* 136 2001: pp. 73 – 79.
13. **Mändl, S., Scholze, E., Neumann, H., Rauschenbach, B.** Nitrogen Diffusivity in Expanded Austenite *Surface and Coatings Technology* 174 – 175 2003: pp. 1191 – 1195.
14. **Christiansen, T. L., Dahl, K. V., Somers, M. A. J.** Nitrogen Diffusion and Nitrogen Depth Profiles in Expanded Austenite: Experimental Assessment, Numerical Simulation and Role of Stress *Materials Science and Technology* 24 2008: pp. 159 – 167.
15. **Christiansen, T. L., Somers, M. A. J.** Low-Temperature Gaseous Surface Hardening of Stainless Steel: the Current Status *International Journal of Materials Research* 100 2009: pp. 1361 – 1377.
16. **Depouhon, P., Sprauel, J. M., Mailhe, M., Mermoz, E.** Mathematical Modeling of Residual Stresses and Distortions Induced by Gas Nitriding of 32CrMoV13 Steel *Computational Materials Science* 82 2014: pp. 178 – 190. http://dx.doi.org/10.1016/j.commatsci.2013.09.043
17. **Öztürk, O., Okur, S., Pichon, L., Liedke, M. O., Riviere, J. P.** Magnetic Layer Formation on Plasma Nitrided CoCrMo Alloy *Surface and Coating Technology* 205 2011: pp. 280 – 285.
18. **Mändl, S., Lutz, J., Díaz, C., Gerlach, J. W., García, J. A.** Influence of Reduced Current Density on Diffusion and Phase Formation During PIII Nitriding of Austenitic Stainless Steel and CoCr Alloys *Surface and Coating Technology* 239 2014: pp. 116 – 122.
19. **Manova, D., Lutz, J., Gerlach, J. W., Neumann, H., Mändl, S.** Relation Between Lattice Expansion and Nitrogen Content in Expanded Phase in Austenitic Stainless Steel and CoCr Alloys *Surface and Coatings Technology* 205 2011: pp. S290 – S293. http://dx.doi.org/10.1016/j.surfcoat.2010.12.046
20. **Xuan, F. Z., Shao, S. S., Wang, Z., Tu, S. T.** Influence of Residual Stress on Diffusion-Induced Bending in Bilayered Microcantilever Sensors *Thin Solid Films* 518 2010: pp. 4345 – 4350.
21. **Zoltowski, P.** Effects of Self-Induced Mechanical Stress in Hydrogen Sorption by Metals, by EIS *Electrochimica Acta* 44 1999: pp. 4415 – 4429. http://dx.doi.org/10.1016/S0013-4686(99)00157-7
22. **Zoltowski, P.** Diffusion of Hydrogen in Self-Stressed Metals – Transfer Function Spectroscopy Approach *Journal of Electroanalytical Chemistry* 501 2001: pp. 89 – 99. http://dx.doi.org/10.1016/S0022-0728(00)00507-6
23. **Galdikas, A., Moskalioviene, T.** Stress Induced Nitrogen Diffusion During of Austenitic Stainless Steel *Computational Materials Science* 50 2010: pp. 796 – 799.
24. **Galdikas, A., Moskalioviene, T.** Modeling of Stress Induced Nitrogen Diffusion in Nitrided Stainless Steel *Surface and Coatings Technology* 205 2011: pp. 3742 – 3746.
25. **Tsuji, S.** Computer Simulation of Multiphase Binary Diffusion in Gas-Solid Type Couples *Materials Transactions* 46 2005: pp. 1248 – 1254. http://dx.doi.org/10.2320/matertrans.46.1248
26. **Christiansen, T., Somers, M. A. J.** Avoiding Ghost Stress on Reconstruction of Stress and Composition – Depth Profiles from Destructive X-ray Diffraction Depth Profiling *Materials Science and Engineering A* 424 2006: pp. 181 – 189.
27. **Okur, S.** Structural, Compositional and Mechanical Characterization of Plasma Nitrided CoCrMo Alloy *A Thesis of Master of Science* Izmir Institute of Technology, Izmir, 2009.
28. **Mischler, S., Munoz, A. I.** Wear of CoCrMo Alloys Used in Metal-on-Metal Hip Joints: a Tribocorrosion Appraisal *Wear* 297 2013: pp. 1081 – 1094.
29. **DeGroot, S, R, Mazur, P.** Non-Equilibrium Thermodynamics. North Holland Publ. Comp., 1962: 452 p.